

Searching for the 1 mHz variability in the flickering of V4743 Sgr: a Cataclysmic Variable accreting at a high rate

A. Dobrotka¹, M. Orio^{2,3}, D. Benka¹ and A. Vanderburg²

¹ Advanced Technologies Research Institute, Faculty of Materials Science and Technology in Trnava, Slovak University of Technology in Bratislava, Bottova 25, 917 24 Trnava, Slovakia

² Department of Astronomy, University of Wisconsin 475 N. Charter Str. Madison, WI 53706

³ INAF - Astronomical Observatory Padova, vicolo dell'Osservatorio 5, 35122 Padova, Italy

Received / Accepted

ABSTRACT

Aims. A few well studied cataclysmic variables (CVs) have shown discrete characteristic frequencies of fast variability; the most prominent ones are around $\log(f/\text{Hz}) \simeq -3$. Because we still have only small number statistics, we obtained a new observation to test whether this is a general characteristic of CVs, especially if mass transfer occurs at a high rate typical for dwarf nova in outbursts, in the so called “high state”.

Methods. We analyzed optical *Kepler* data of the quiescent nova and intermediate polar V4743 Sgr. This system hosts a white dwarf accreting through a disk in the high state. We calculated the power density spectra, and searched for break or characteristic frequencies. Our goal is to assess whether the mHz frequency of the flickering is a general characteristic.

Results. V4743 Sgr has a clear break frequency at $\log(f/\text{Hz}) \simeq -3$. This detection increases the probability that the mHz characteristic frequency is a general feature of CVs in the high state, from 69% to 91%. Furthermore, we propose the possibility that the variability is generated by similar mechanism as in the nova-like system MV Lyr, which would make V4743 Sgr unique.

Key words. accretion, accretion discs - stars: novae, cataclysmic variables - stars: individual: V4743 Sgr

1. Introduction

Cataclysmic variables (CVs) are interacting binaries powered by an accretion process. The mass is transferred from a main sequence companion star and falls onto the white dwarf (WD). In the absence of a strong magnetic field, an accretion disc forms. CVs are divided into subclasses based on characteristic variability features. Dwarf novae (DN) show quasi-regular outbursts lasting several days, repeated on time scales of 10 - 100 days (see Warner 1995 for review). Nova-like binaries, especially the VY Scl systems, spend most of their lifetime in a “high state” in which the accretion rate \dot{m}_{acc} is so high that DN outbursts are suppressed. The exact value of \dot{m}_{acc} depends on the rest of the physical parameters of the system, but is generally around a few $10^{-10} M_{\odot} \text{ yr}^{-1}$. Most classical novae in the years immediately after an outburst may also be in a stage of enhanced mass transfer, while they may be “hibernating” for most of the period between outbursts (Hillman et al. 2020). Both classes of objects, VY Scl and novae, seem to have stable accretion disks and are good targets to study the accretion process.

The disc instability model explains the dwarf nova cycle (see Lasota 2001 for a review). The DN outbursts are caused by a viscous-thermal instability triggered by changes in the ionization state of hydrogen while matter flows through the disc (Hōshi 1979, Meyer & Meyer-Hofmeister 1981, Lasota 2001). Thus there are two basic states, recurring in a limit

cycle: the high state (DN outbursts) when \dot{m}_{acc} through the disc increases, and the low state with lower \dot{m}_{acc} (quiescence; see Osaki 1974 for the original idea). The accretion disc is fully developed up to the WD in the high state, while it is truncated in the low one. The high state is optically brighter than the low state.

The fast stochastic variability, which we call flickering, is a typical manifestation of the underlying accretion process. The three most important observational characteristics of the flickering are; 1) linear correlation between variability amplitude and log-normally distributed flux (so called rms-flux relation) observed in all accreting systems (see Scaringi et al. 2012b, Van de Sande et al. 2015 for CVs), 2) power density spectra (PDS) in the shape of a red noise or band limited noise with characteristic frequencies (Scaringi et al. 2012a, Dobrotka et al. 2014, Dobrotka et al. 2016 describe how this occurs in CVs) and 3) time lags, in which the flares reach their maxima slightly earlier in the blue than in the red (Scaringi et al. 2013, Bruch 2015).

In the light curves of several CVs, characteristic frequencies have been identified in the PDSs. Ground observations in the optical range have usually shown a single break frequency like in UU Aqr (Baptista & Bortoletto 2008) and KR Aur (Kato et al. 2002). Detecting multiple PDS components requires light curves obtained in long exposures. These were provided by the *Kepler* satellite for MV Lyr (Scaringi et al. 2012a), V1504 Cyg (Dobrotka & Ness 2015) and V344 Lyr (Dobrotka et al. 2016). Additional observations with *XMM-Newton* in the

Send offprint requests to: A. Dobrotka, e-mail: andrej.dobrotka@stuba.sk

X-ray range have allowed detection of the same frequencies detected in optical in MV Lyr (Dobrotka et al. 2017) and possibly in V1504 Cyg (Dobrotka et al., in preparation). Other systems like VW Hyl, WW Cet and T Leo were observed in X-rays, revealing a single characteristic frequency (Balman & Revnivtsev 2012) or multiple components in SS Cyg (Balman & Revnivtsev 2012) or RU Peg (Dobrotka et al. 2014).

Dobrotka et al. (2020) summarized all these detections, suggesting that two characteristic frequencies can exist in the low state, with an additional and most prominent frequency with $\log(f/\text{Hz}) \simeq -3$ in the high state. However, this suggestion was based on only 12 detections. The frequency distribution can be easily explained by the random appearance of a uniform distribution. More detections are needed to construct a significant histogram, which is the aim of this paper.

The flickering phenomenon and its frequencies, in fact, bear direct evidence of the accretion mode. Scaringi (2014) interpreted the main feature at $\log(f/\text{Hz}) \simeq -3$ in the PDS calculated from *Kepler* data of MV Lyr as due to a hot, geometrically thick disc (hot X-ray corona), surrounding a cool, geometrically thin disc. The propagating mass accretion fluctuations (Lyubarskii 1997, Kotov et al. 2001, Arévalo & Uttley 2006) in the corona generate X-ray variability with characteristic frequency of $\log(f/\text{Hz}) \simeq -3$. The X-rays are reprocessed by the geometrically thin disc into optical variability.

Dobrotka et al. (2017) further elaborated this model on the basis of observations, proposing that two different regions in a CV may emit X-rays, not just the boundary layer as it is usually assumed. One region is the standard boundary layer between the geometrically thin disc and the WD, the second must be the boundary between the geometrically thick corona and the WD, or the corona itself.

However, the ratio of X-ray to optical luminosity is of the order of 0.1 (see e.g. Dobrotka et al. 2020), which is too low to explain the observed optical and UV variability. Dobrotka et al. (2019) studied the shot profile of the flickering in the *Kepler* data of MV Lyr, finding high and low amplitude components with frequencies close to $\log(f/\text{Hz}) \simeq -3$. The small amplitude one can be indeed explained with the reprocessing scenario (see also Dobrotka et al. 2020). The variability is attributed to two separate sources: the geometrically thin disc, and the reprocessed X-rays of the geometrically thick corona.

2. V4743 Sgr and the new observations

In this study, we analyse the variability of a CV system that does not show DN outbursts, and for several reasons is very likely to be found in a high state (that is, with a hot and ionized disk); the recent nova V4743 Sgr (Nova Sgr 2002c).

V4743 Sgr was discovered in outburst in September 2002 by Haseda et al. (2002). While it was still in outburst and had turned into a luminous supersoft X-ray source, Ness et al. (2003) found variability with a 0.75 mHz frequency in *Chandra* data taken 180 days after optical maximum. More detailed analyses of these *Chandra* data and of *XMM-Newton* X-ray data taken 196 days after maximum were later presented by Leibowitz et al. (2006) and Dobrotka & Ness (2010). The 0.75 mHz variation was also still present in X-rays even at quiescence, as late as day

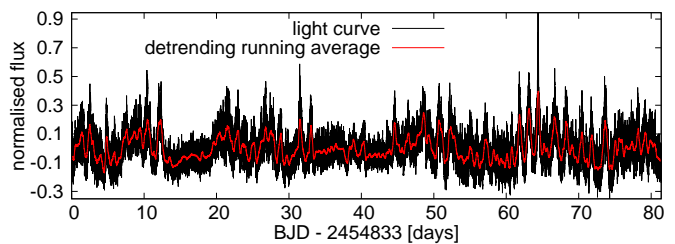


Fig. 1. *Kepler* light curve of V4743 Sgr. The flux has been normalised by dividing by the median flux of the observation. The time is in standard *Kepler* time.

1286 after maximum. However, this dominant feature was double peaked in nature in the observations taken 180 and 196 days after the outburst.

Kang et al. (2006) presented ground optical photometry and detected two periods of 6.7 hr and ~ 24 min. The authors attributed the lower frequency signal to the orbital period and, assuming that the 0.75 mHz signal (22 min) present in X-rays is the rotation period of the central WD, the optical period of 24 min was interpreted as the beat period between the orbital and rotation period of the WD, respectively. This interpretation was confirmed by Zemko et al. (2018) by analysing the *Kepler* light curve.

Detection of the rotation period in X-rays suggests an intermediate polar (IP) nature of V4743 Sgr. Zemko et al. (2016) analyzed the X-ray observations they had taken at quiescence. The X-ray spectra did have characteristics in common with known IPs, with thermal plasma and a partially covering absorber, and a supersoft blackbody-like component, possibly originating from the polar regions irradiated by an accretion column.

The enigmatic double peak nature of the main feature at 0.75 mHz was resolved by Dobrotka & Ness (2017). Using simulations, these authors showed that the double peak is produced by a single frequency of 0.75 mHz with variable amplitude.

V4743 Sgr has not shown DN outbursts during *Kepler* monitoring (Zemko et al. 2018) and is likely to be in the enhanced mass transfer rate predicted by the hibernation scenario, with the disc of V4743 Sgr in a hot and ionized high state. The binary was in Field 7 of the *Kepler* telescope (Borucki et al. 2010) during the K2 mission between 2015 Oct 04 and 2015 Dec 26, so we requested to obtain data (EPIC 216631947) with the short cadence in which the spacecraft saved and downloaded images of the target every 58.85 seconds, as opposed to *Kepler*'s usual 29.4 minute “long cadence” sampling rate.

The *Kepler* light curve is shown in Fig. 1. Before the flux normalisation, systematic corrections were applied¹. The data were barycentre corrected.

While the “long cadence” data allowed detection of the beat period between the orbital and the rotation period (Zemko et al. 2018), with the “short cadence” we wanted to study in detail the flickering feature of this recent nova returned in quiescence, which is also an IP. An interesting question is whether IPs, with their truncated disks, sat-

¹ The *Kepler* team estimates the contribution of scattered background light and subtracts that off. The background is a large source of photon noise, so in some cases with faint stars, where the background is much larger than the flux from the star, the estimated brightness may be negative in some cases.

isfy disc conditions for the scenario described above and whether we can expect to detect similar characteristic frequencies of flickering.

The truncation of the inner disc is generated by a magnetic pressure balancing the ram pressure of the accretion flow. This defines a magnetospheric radius

$$r_m = 9.8 \times 10^8 \left(\frac{\dot{m}_{\text{acc}}}{10^{15} \text{ g s}^{-1}} \right)^{-2/7} m_1 \left(\frac{\mu}{10^{30} \text{ G cm}^3} \right)^{4/7} \text{ cm}, \quad (1)$$

where m_1 is the WD mass and μ is the magnetic moment of the WD. If the mass transfer rate in post-novae is enhanced, this enhances the mass accretion rate \dot{m}_{acc} . When \dot{m}_{acc} is larger, r_m is smaller. Equation (1) describes how the inner disc truncation at r_m decreases if the \dot{m}_{acc} parameter rises keeping all other values like m_1 and μ fixed.

However, V4743 Sgr is quite a special case. If \dot{m}_{acc} in post-novae is enhanced, it can be 3 order of magnitudes (10^{-8} vs. $10^{-11} \text{ M}_{\odot} \text{ yr}^{-1}$) larger than in the average IP in which the disc truncation is large. The decrease of the truncation radius r_m can be large. Based on Equation (1) it can reach 14% of the value with quiescent \dot{m}_{acc} . It is difficult to establish whether this makes the accretion disc similar to non-magnetic systems, but we suggest that V4743 Sgr is unlikely to be an IP with a large inner disc radius.

3. PDS analysis

3.1. Method

V4743 Sgr was observed for a long time, allowing a more detailed time evolution study, therefore we studied separately each consecutive 10-day time interval. For the PDS study we divided each 10 day light curve into 10 subsamples, and using the Lomb-Scargle algorithm (Scargle 1982) normalised by the total variance (Horne & Baliunas 1986) we calculated log-log periodogram for each of these subsamples. We divided these periodograms into equally spaced bins of 0.05 dex, and averaged all periodogram values within these bins in order to get the mean power p . The only condition was to include at least 20 periodogram points per bin in order to have a Gaussian distribution. The averaging is performed over $\log(p)$ rather than p following Papadakis & Lawrence (1993), and such averaging yields symmetric errors (see e.g. van der Klis 1989, Aranzana et al. 2018). The PDS low frequency end is defined by the duration of each light curve subsample while the high frequency end is set by the Nyquist frequency.

3.2. Results

We downloaded the short-cadence pixel data from the Mikulski Archive for Space Telescopes (MAST²). We extracted the light curve and removed systematics due to the spacecraft's drift³ following Vanderburg & Johnson (2014) and Vanderburg et al. (2016).

The light curve in Fig. 1 shows obvious variability on a time scale of about a day. Flare-like phenomena follow one

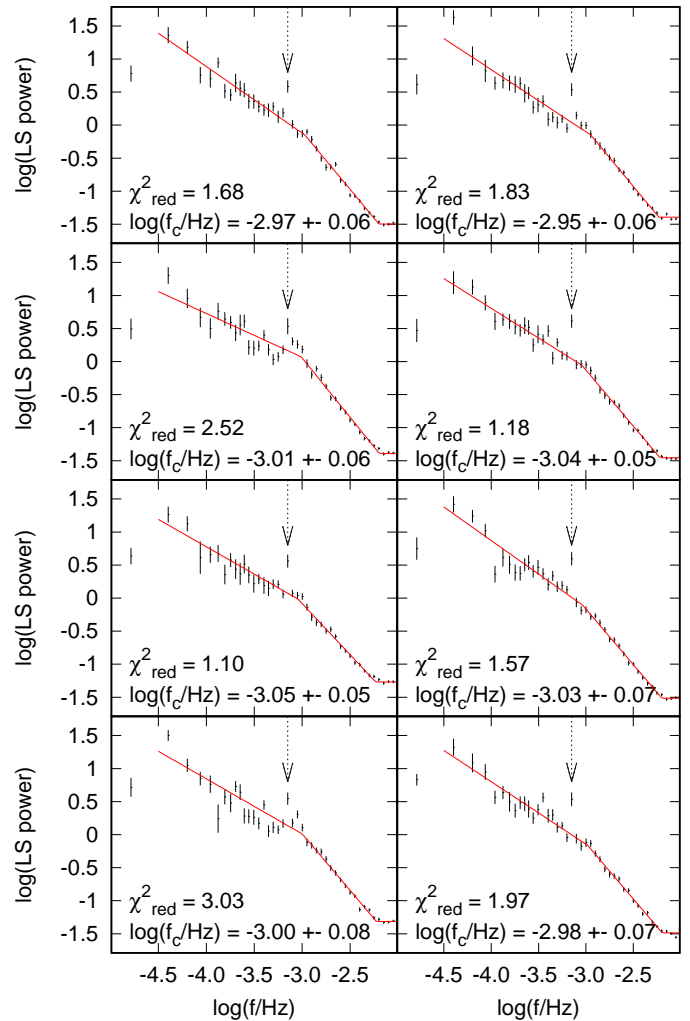


Fig. 2. PDSs of V4743 Sgr with three component fits (red lines). Eight cases are shown, because the light curve is divided into eight subsamples with duration of 10 days. Each PDS point is displayed as a vertical line showing the uncertainty interval. The latter represents the standard error of the mean. The labels report the reduced χ^2 indicating the goodness of the fits, and the characteristic break frequencies f_c . The vertical dashed arrows show the frequency related to the WD spin period, which was excluded from the fitting process. The PDS point with the lowest frequency is not included in the fit, because the considerably lower power is a result of detrending.

another or are separated by constant flux intervals. In order to analyse equivalent data subsamples (with the same long-term trend) we detrended the light curve with a running average using 401 points in the running window⁴.

Dividing the V4743 Sgr light curve into 10 day long subsamples yielded eight PDSs depicted in Fig. 2. All PDSs show the same shape with red noise up to $\log(f/\text{Hz}) \simeq -2.2$. Higher frequencies are dominated by the Poisson noise. However, a change of the red noise slope is obvious in all cases near $\log(f/\text{Hz}) \simeq -3.0$. This region shows also one bin with considerably higher power which represents the optical signal related to the WD spin detected by Kang et al. (2006).

² https://archive.stsci.edu/k2/search_retrieve.html

³ The drift is generated by inability of the spacecraft to maintain precise pointing due to reaction wheels failure. The telescope re-points itself on timescales of 6 hours.

⁴ 200 points to the left, 200 points to the right and the detrended point itself.

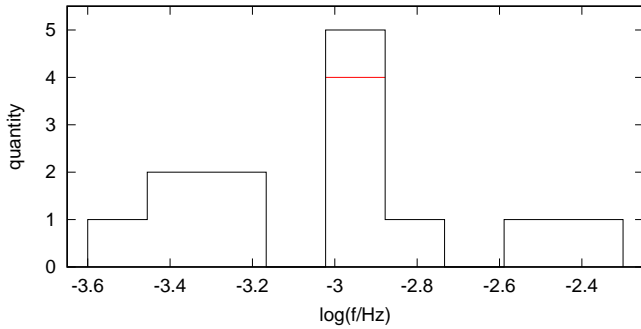


Fig. 3. Histogram of the measured break/characteristic frequencies in the high state of CVs (from Dobrotka et al. 2020, after including V4743 Sgr. The red line represents the original version.

In order to search for the characteristic break frequency f_c , we fitted the PDSs with a broken power law model consisting of two linear functions $\log(p) = a \log(f) + b$ and a constant $\log(p)$. The linear functions are connected at f_c and the constant represents the Poisson noise at the highest frequencies. The optical signal related to the WD spin, and the lowest frequency PDS point affected by the detrending were excluded from the fitting process. The resulting f_c values are summarized in Fig. 2. The weighted mean of all eight values is -3.01 ± 0.02 .

4. Discussion

4.1. The significance of the new measurement

In this paper we studied the optical fast variability of a CV system, V4743 Sgr that is likely to be in a high state and to have a hot ionized disc. We searched for characteristic frequencies in the PDSs and found a value of $\log(f/\text{Hz}) \simeq -3.01$.

Dobrotka et al. (2020) summarized all the detected characteristic frequencies in CVs in optical and X-rays. They collected 12 values, and the resulting histogram (Fig. 3) shows discrete values with dominant concentration of frequencies around $\log(f/\text{Hz}) \simeq -3$. However, a number of 12 is too low for a significant conclusion. In this work, we increased the number of detections to 13. The histogram feature at $\log(f/\text{Hz}) \simeq -3$ now shows 5 values compared to 4 in the histogram of Dobrotka et al. (2020).

In order to test the probability of the histogram shape being due to a random process, we performed a simulation test. We randomly selected 12 values using a uniform distribution, and we calculated the corresponding histogram. After one million simulations we found that 31.4% of the simulations produced a peak at value 4 or higher. Therefore, the probability that CVs show a typical characteristic frequency at $\log(f/\text{Hz}) \simeq -3$ before this study was only 68.6%. Including the V4743 Sgr case studied in this paper, the total number of detected frequencies increased to 13 with a maximum number of systems in the histogram of 5, at $\log(f/\text{Hz}) \simeq -3$. This increased the confidence of the statement to 90.9%.

With only one additional measurement of frequency we thus transformed an uncertain idea into a much more statistically significant result.

4.2. Origin of the flickering in V4743 Sgr

The root cause of the variability in V4743 Sgr is not straightforward to understand. The source of X-ray variability with $\log(f/\text{Hz}) \simeq -3$ in the well studied system MV Lyr can be either the hot X-ray corona, or the boundary layer between the corona and the WD, and it is hard to distinguish between the two cases. However, V4743 Sgr is an IP, which means that it does not have a boundary layer. The common structure in both systems is the geometrically thick corona surrounding the geometrically thin disc.

Magnetic CVs have truncated discs, and the inner disc edge generates the time scales of the variability. The observed f_c in IPs are very close to $\log(f/\text{Hz}) \simeq -3$ or higher (Revnivtsev et al. 2010, Semena et al. 2014). Usually, f_c in the corresponding PDSs are close to the spin frequency of the WD (P_{spin}) yielding $f_c \times P_{\text{spin}} \simeq 1$. This is observed in our PDS of V4743 Sgr with $f_c \times P_{\text{spin}} \simeq 1.3$. The same behaviour is seen also in X-ray pulsars, with a neutron star as a central compact object (Revnivtsev et al. 2009). The relation between f_c and P_{spin} is explained by corotating central objects and inner disc edges. The latter has Keplerian frequency as f_c .

However, V4743 Sgr is a post nova system, so \dot{m}_{acc} may be higher compared to standard IPs. The characteristic frequencies during higher \dot{m}_{acc} episodes shows $f_c \times P_{\text{spin}} > 10$ like in the case of X-ray pulsar A0535+26 (Revnivtsev et al. 2010). The IP V1223 Sgr also shows $f_c \times P_{\text{spin}} > 10$ (Revnivtsev et al. 2010). This means that the characteristic (Keplerian) frequency at the truncation radius is considerably higher than the Keplerian frequency at the corotating radius. The same is suggested for V4743 Sgr if we assume that it has higher \dot{m}_{acc} (Section 2). For this particular system the condition $f_c \times P_{\text{spin}} > 10$ yields considerably higher f_c than $\log(f/\text{Hz}) \simeq -3$, and the detected f_c must be explained by another mechanism.

Therefore, we conclude that the detected $\log(f_c/\text{Hz}) \simeq -3$ in V4743 Sgr is generated at the inner disc edge like in IPs, or by the central disc region with geometrically thick X-ray corona like in MV Lyr.

4.3. V4743 Sgr long-term variability

The light curve of this quiescent nova shown in Fig. 1 exhibits clear variability on a time scale of about one day. Similar variability has been observed in VY Scl systems when the disc is in the high state, specifically in V794 Aql (Honeycutt et al. 1994, Honeycutt & Robertson 1998) and FY Per (Honeycutt 2001). In V794 Aql, either the flares are due to disc instabilities when mass transfer from the secondary temporarily ceases (Honeycutt et al. 1994), or, more likely, the disc remains in the high state while the variability is due to mass transfer variations from the secondary (Honeycutt & Robertson 1998). Such variability on time scale of a day is never observed in known DN systems.

We also observed no DN outbursts during the 83 days of the *Kepler* observation. Standard IPs also do not show DN outbursts, but following disc instability model these are stabilised in the low cold state by the WD magnetic field and low \dot{m}_{acc} (Hameury & Lasota 2017). Contrary, V4743 Sgr has characteristics that are much more typical of CVs accreting at high \dot{m}_{acc} than of standard IPs or DN systems.

5. Summary and conclusions

We analysed the *Kepler* observation of the post-nova V4743 Sgr, which is very likely to be accreting in the high state. We studied the fast stochastic variability (flickering) and found a characteristic frequency near $\log(f/\text{Hz}) \simeq -3$ in the corresponding PDSs. We thus increase the number of detections of this characteristic frequency, and obtained further evidence that all CVs in the optical high state show this flickering frequency, as recently proposed by Dobrotka et al. (2020). The confidence of this statement was 69% before the new data analysis contained in this paper. It increased now to 91%, making this phenomenological evidence much more interesting and worth of further studies.

Finally, we found that the intermediate polar V4743 Sgr is probably accreting at a higher mass accretion rate than standard intermediate polars. The accretion disc of the former should be hot with ionised hydrogen, while the latter have cold discs with neutral hydrogen (Hameury & Lasota 2017). Therefore, V4743 Sgr is similar to nova-like systems, and the source of the flickering has a different origin compared to standard intermediate polars (Revnivtsev et al. 2010). This would be one of those rare cases in which the flickering originates in the central portion of the disk with a hot X-ray corona (Scaringi 2014) like in MV Lyr (Scaringi 2014, Dobrotka et al. 2020).

Acknowledgement

AD was supported by the Slovak grant VEGA 1/0408/20, and by the Operational Programme Research and Innovation for the project : Scientific and Research Centre of Excellence SlovakION for Material and Interdisciplinary Research⁴, code of the project ITMS2014+ : 313011W085 co-financed by the European Regional Development Fund.

References

- Aranzana, E., K rding, E., Uttley, P., Scaringi, S., & Bloemen, S. 2018, MNRAS, 476, 2501
- Ar valo, P. & Uttley, P. 2006, MNRAS, 367, 801
- Balman, S. & Revnivtsev, M. 2012, A&A, 546, A112
- Baptista, R. & Bortoletto, A. 2008, ApJ, 676, 1240
- Borucki, W. J. et al. 2010, Science, 327, 977
- Bruch, A. 2015, A&A, 579, A50
- Dobrotka, A., Mineshige, S., & Ness, J.-U. 2014, MNRAS, 438, 1714
- Dobrotka, A., Negoro, H., & Konopka, P. 2020, A&A, 641, A55
- Dobrotka, A., Negoro, H., & Mineshige, S. 2019, A&A, 631, A134
- Dobrotka, A. & Ness, J.-U. 2010, MNRAS, 405, 2668
- Dobrotka, A. & Ness, J.-U. 2015, MNRAS, 451, 2851
- Dobrotka, A. & Ness, J. U. 2017, MNRAS, 467, 4865
- Dobrotka, A., Ness, J.-U., & Baj          , I. 2016, MNRAS, 460, 458
- Dobrotka, A., Ness, J.-U., Mineshige, S., & Nucita, A. A. 2017, MNRAS, 468, 1183
- H shi, R. 1979, Progress of Theoretical Physics, 61, 1307
- Hameury, J. M. & Lasota, J. P. 2017, A&A, 602, A102
- Haseda, K., West, D., Yamaoka, H., & Masi, G. 2002, IAU Circ., 7975, 1
- Hillman, Y., Shara, M. M., Prialnik, D., & Kovetz, A. 2020, Nature Astronomy, 4, 886
- Honeycutt, R. K. 2001, PASP, 113, 473
- Honeycutt, R. K., Cannizzo, J. K., & Robertson, J. W. 1994, ApJ, 425, 835
- Honeycutt, R. K. & Robertson, J. W. 1998, AJ, 116, 1961
- Horne, J. H. & Baliunas, S. L. 1986, ApJ, 302, 757
- Kang, T. W., Retter, A., Liu, A., & Richards, M. 2006, AJ, 132, 608
- Kato, T., Ishioka, R., & Uemura, M. 2002, PASJ, 54, 1033
- Kotov, O., Churazov, E., & Gilfanov, M. 2001, MNRAS, 327, 799
- Lasota, J. 2001, New A Rev., 45, 449

- Leibowitz, E., Orio, M., Gonzalez-Riestra, R., et al. 2006, MNRAS, 371, 424
- Lyubarskii, Y. E. 1997, MNRAS, 292, 679
- Meyer, F. & Meyer-Hofmeister, E. 1981, A&A, 104, L10
- Ness, J., Starrfield, S., Burwitz, V., et al. 2003, ApJ, 594, L127
- Osaki, Y. 1974, PASJ, 26, 429
- Papadakis, I. E. & Lawrence, A. 1993, MNRAS, 261, 612
- Revnivtsev, M., Burenin, R., Bikmaev, I., et al. 2010, A&A, 513, A63
- Revnivtsev, M., Churazov, E., Postnov, K., & Tsygankov, S. 2009, A&A, 507, 1211
- Scargle, J. D. 1982, ApJ, 263, 835
- Scaringi, S. 2014, MNRAS, 438, 1233
- Scaringi, S., K rding, E., Groot, P. J., et al. 2013, MNRAS, 431, 2535
- Scaringi, S., K rding, E., Uttley, P., et al. 2012a, MNRAS, 427, 3396
- Scaringi, S., K rding, E., Uttley, P., et al. 2012b, MNRAS, 421, 2854
- Semena, A. N., Revnivtsev, M. G., Buckley, D. A. H., et al. 2014, MNRAS, 442, 1123
- Van de Sande, M., Scaringi, S., & Knigge, C. 2015, MNRAS, 448, 2430
- van der Klis, M. 1989, in NATO Advanced Science Institutes (ASI) Series C, Vol. 262, NATO Advanced Science Institutes (ASI) Series C, ed. H. Ogelman & E. P. J. van den Heuvel, 27
- Vanderburg, A. & Johnson, J. A. 2014, PASP, 126, 948
- Vanderburg, A., Latham, D. W., Buchhave, L. A., et al. 2016, ApJS, 222, 14
- Warner, B. 1995, Cambridge Astrophysics Series, 28
- Zemko, P., Ciroi, S., Orio, M., et al. 2018, MNRAS, 480, 4489
- Zemko, P., Orio, M., Mukai, K., et al. 2016, MNRAS, 460, 2744